NUKLEONIKA 2006;51(2):125–129

ORIGINAL PAPER

Gamma-ray beam attenuation to assess the influence of soil texture on structure deformation

Luiz F. Pires,
Osny O. S. Bacchi,
Nivea M. P. Dias

Abstract Gamma-ray beam attenuation is a non-invasive technique that permits analysis of soil porosity without disturbing the region of interest of the core sample. The technique has as additional advantage to allow measurements point by point on a millimetric scale in contrast to other methodologies that are invasive and analyze the soil properties in the bulk sample volume. Soil porosity can be used as an important parameter to quantify soil structural damages, which affect soil aeration, water movement and retention. In this study, porosities of three soils different in texture were measured at various positions in order to analyze the impact of the sampling procedure on the structure of each particular soil texture. The gamma-ray attenuation system consisted of an ^{241}Am radioactive source having an activity of 3.7 GBq, collimated with cylindrical lead collimators of 2 mm diameter. The results obtained show the presence of dense regions near the edges of samples and that different soil textures can suffer distinct deformations at sampling.

Key words gamma-ray attenuation • soil physical properties • soil structure deformation • soil sampling • soil porosity • applied nuclear physics

L. F. Pires✉, O. O. S. Bacchi, N. M. P. Dias
Center for Nuclear Energy in Agriculture,
The University of São Paulo,
C. P. 96, C. E. P. 13.400-970, Piracicaba, SP, Brazil,
Tel.: +55 19 3429 4600 ext. 4712,
Fax: +55 19 3429 4610,
E-mail: lfpires@cena.usp.br

Received: 3 November 2005
Accepted: 22 February 2006

Introduction

Soil sample quality is directly related to soil structure, which is one of the most important properties that influences root development, water and gas movement and retention, soil fauna, etc. [11]. An important parameter that has been increasingly used to quantify soil structural changes is its porosity, which affects many of the important processes in soils and gives an insight on other soil properties, e.g. soil bulk density (ρ_s) [9]. Its measurement is also important for aspects related to soil water content (θ) as well as for estimation of the soil volume available for water and gas movement.

In a previous study, Pires *et al.* [13] evaluated the impact of different cylinder sizes on the structure of a sandy soil, showing that the length and diameter of the sample is very important in soil physics measurements, and that small samples, certainly have great probability to give incorrect or non-representative results [16]. However, the literature concerning the effect of sampling devices on the structure of soils of different textures is scarce. Information regarding the effect of sampler devices are not only important to select the best ones, but also to call attention of the soil physicists about the importance of the sample structure quality used on measurements of soil physical parameters.

An accurate, fast, and non-destructive inspection technique, e.g. gamma-ray attenuation (GRA) could be an interesting alternative to reliably determine physical deformations on the structure of a soil sample.

This technique allows measurements of soil porosity point by point on a millimetric scale without interfering with the physical integrity of the sample [15]. GRA technique was first introduced into soil science by Vomocil [17] for soil bulk density analysis. The application of GRA in soil physics has been largely discussed in the literature [2, 3, 10].

The objectives of this study were to investigate the sensibility of the gamma-ray attenuation technique as a method for assessing the structural deformations to soils having different textures and to indicate which type of soil texture suffers the lowest impact at sampling.

Theory

When a gamma-ray beam passes through a material with an infinitesimal thickness, *dx*, different electromagnetic processes occur, decreasing the number of transmitted photons N (number of photons $\cdot m^{-2} \cdot s^{-1}$). If N_0 photons per second are incident in the atoms composing the material and have a probably of interaction μ (cm^{-1}), the number of photons, dN, which have not interact is:

$$dN = -\mu N dx \tag{1}$$

where the proportionality constant μ is called the linear attenuation coefficient. It measures the photon absorption or scatter probability per unit length while interacting within the sample. For a piece of material of finite thickness x (cm) and using appropriate boundary conditions, the integration of Eq. (1) shows that the intensity of photons that have not suffered interactions, follow the Beer-Lambert law [8].

According to the Beer-Lambert law, a narrow beam linear attenuation coefficient is given by

$$\mu = \left[\frac{1}{x} \cdot \ln\left(\frac{N_0}{N}\right)\right] \tag{2}$$

A coefficient more accurately characterizing a given material is the density independent mass attenuation coefficient μ/ρ ($cm^2 \cdot g^{-1}$):

$$\frac{\mu}{\rho} = \left[\frac{1}{\rho \cdot x} \cdot \ln\left(\frac{N_0}{N}\right)\right] \tag{3}$$

Material and methods

Soil sampling

Core samples were collected from profiles of three soils, different in texture, characterized as: Geric Ferralsol (66% sand, 6% silt, 28% clay – soil 1), Eutric Nitosol (24% sand, 33% silt, 43% clay – soil 2), and Rhodic Ferralsol (26% sand, 26% silt, 48% clay – soil 3) at experimental fields in Piracicaba, Brazil (22°40' S; 47°38' W; 580 m a.s.l.). Nine cylindrical samples (h = 3.0 cm, D = 4.8 cm, $V \approx 55$ cm^3), three from each soil, were collected at the soil surface with aluminum cylinders. At the location selected for sampling the vegetation and any other material were removed from the soil surface. To collect the soil samples a steel cylinder was attached to the aluminum cylinder (Figs. 1a and 1b) and both were placed into the surface of the soil. To push the cylinders

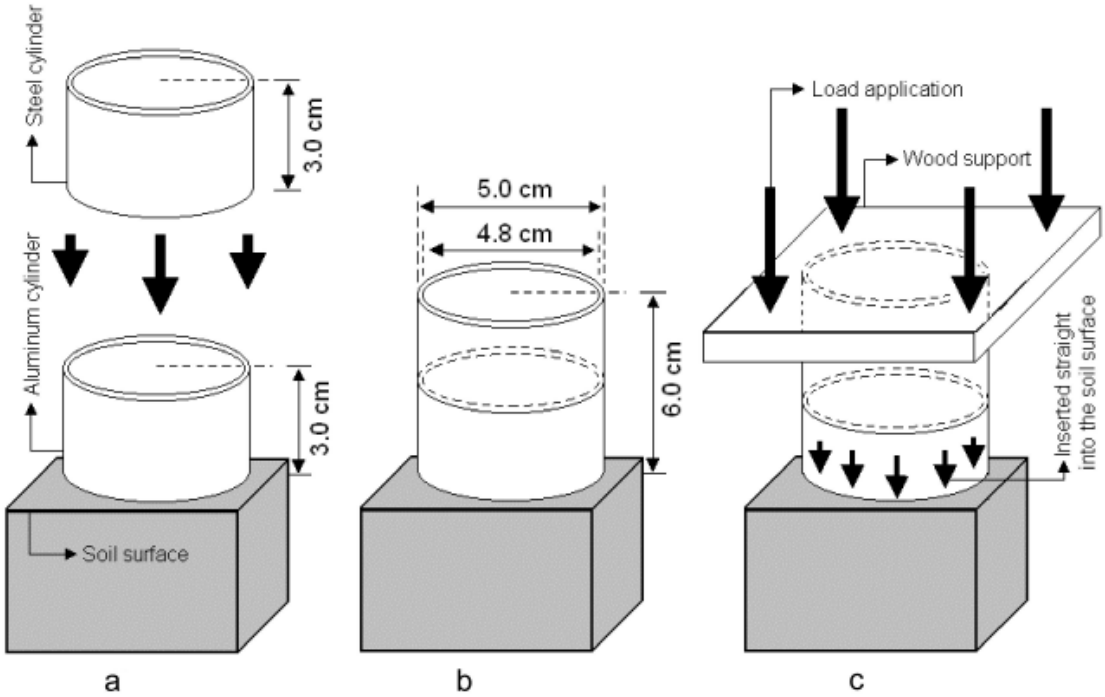

Fig. 1. Schematic diagram of the sampling procedure: (a) aluminum and steel cylinders; (b) steel and aluminum cylinders attachment and (c) soil sample collection. Drawing is schematic and not to scale.

into the soil a piece of wood was placed over the steel cylinder (Fig. 1c) and hit with a rubber hammer in order to spread the force of the hammer blow to all edges of the aluminum cylinder at once. The aluminum cylinder was pushed into the soil to a depth between 4.0 and 8.0 cm. After complete insertion of the cylinders, the surrounding soil was carefully removed to minimize the soil disturbance due to vibration, shear stress and compaction. The excessive soil was carefully trimmed off and top and bottom surfaces of the sample were made flat.

Instrumentation and experimental set-up

The soil porosity was monitored using a radioactive gamma-ray source of ^{241}Am having an activity of 3.7 GBq emitting monoenergetic photons of 59.54 keV. The detector was a 7.62 × 7.62 cm NaI(Tl) scintillation crystal coupled to a photomultiplier tube. Circular lead collimators were adjusted and aligned between source (D = 2 mm) and detector (D = 4.5 mm). As the source and the detector are fixed, the soil sample was moved across the beam and scanned at seven different positions (0.41, 1.04, 1.76, 2.55, 3.32, 4.04, and 4.66 cm) using a steep motor controlled by a microcomputer. A schematic diagram of the experimental set-up is presented in Fig. 2. The radioactive source and detector were mounted 22.0 cm apart and the attenuation coefficients were taken in the vertical planes that included the axes of the cylinders. Counting time was 30 s with three replicates for each position (P).

Data analysis

The measurement of the soil sample porosity by the GRA technique was made using the following equation [12]:

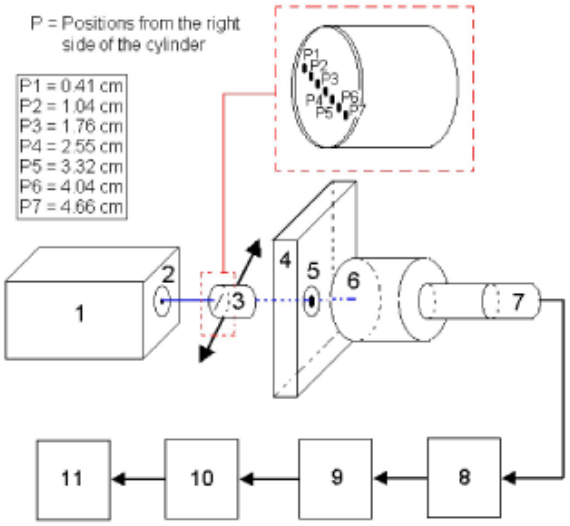

Fig. 2. Schematic diagram of the experimental apparatus: 1 – Pb castle; 2 – ^{241}Am source; 3 – soil sample; 4 – Pb wall; 5 – lead collimator; 6 – NaI(Tl) detector; 7 – photomultiplier; 8 – high-voltage unit; 9 – amplifier; 10 – single-channel analyzer; 11 – counter and timer. Drawing is schematic and not to scale.

$$\phi = \left(1 - \frac{\mu_s}{\mu_p}\right) \cdot 100 \quad (4)$$

where ϕ represents the percent total porosity, μ_p and μ_s are the linear attenuation coefficients at the particle density (ρ_p) and over the bulk soil sample cross section, respectively.

For the evaluation, of μ_s air-dried soil was passed through a 2.0 mm sieve and packed into a thin wall acrylic container (10 × 10 × 10 cm). The intensities of monoenergetic photons were measured in different positions of the soil into the container. The linear attenuation coefficient determined represents an arithmetic mean value of twenty repetitions for each soil and it was obtained from Eq. (2).

The linear attenuation coefficient value for each soil at the particle density depends on a linear relationship between μ_s and ρ_s obtained using artificially compacted soil samples (five different soil bulk density values) packed in acrylic plastic containers [10]. The value of μ_p was calculated by extrapolating the equation for linear regression of μ_s and ρ_s to the value of the particle density for each soil. Details about the method used to measure ρ_p can be found in Flint and Flint [4]. The procedure used to compute the standard error of estimation, the confidence intervals of the slope of the regression line, and the standard error of μ_p determined from the regression model has been described by Helsel and Hirsch [6].

Results and discussion

The mass attenuation coefficients measured were 0.24191 ± 0.00301 (soil 1), 0.31405 ± 0.00288 (soil 2), and 0.29535 ± 0.00340 $cm^2 \cdot g^{-1}$ (soil 3). These values are in accordance with those found in the literature for Brazilian soils [3].

The linearity between the linear attenuation coefficient and bulk density of the soils are shown in Fig. 3.

As can be seen from Fig. 3, all soils demonstrate a linear change in attenuation coefficient with increase in bulk density. The high correlation coefficient (r^2) of the soils was essential for obtaining values of μ_p with a great accuracy and represents a good response of the gamma-ray system for providing reliable values of soil porosity. A larger r^2 among soils should be related to differences in the compaction procedure, which probably caused heterogeneities among compacted layers into the acrylic container packed with soils 2 and 3. The slope of the linear regression between μ_s and ρ_s varied slightly and probably occurs as a result of the differences in atomic composition of the soils [1]. Soil 2 presented the largest slope value and soil 1 the smallest. The larger value of the slope for soil 2 indicates that for a very same soil bulk density increment ($\Delta\rho$) this soil presents the largest variations of $\Delta\mu$. As a consequence, small changes in ϕ for soil 2 can be determined with more assurance than for the other two soils due to the error ($\sigma\phi$) associated to the uncertainty of the radioactive decay process [3].

The results of ρ_p and μ_p, estimated through the extrapolation of the regression lines to values of particle

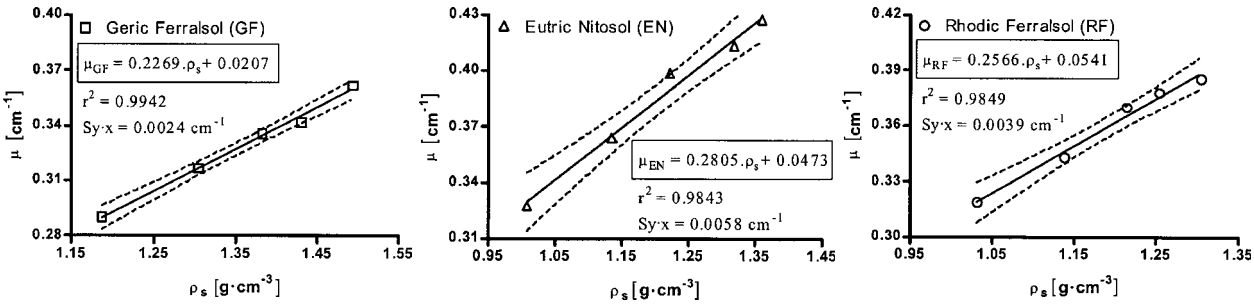

Fig. 3. Relation between linear attenuation coefficient and soil bulk density for the soils. *Sy·x* represents the standard error of estimation.

Table 1. Soil particle densities and gamma-ray linear attenuation coefficients estimated through the extrapolation of the regression lines to values of particle density of the studied soils

Soil order	ρ_p [g·cm^{-3}]*	μ_p [cm^{-1}]**
Geric Ferralsol	2.55 ± 0.02	0.59930 ± 0.06945
Eutric Nitosol	2.68 ± 0.01	0.79897 ± 0.11431
Rhodic Ferralsol	2.54 ± 0.03	0.70602 ± 0.11537

* The standard deviation of ρ_p represents the scatter of five repetitions.
** The standard error of μ_p was determined from the regression model [6].

density, are presented in Table 1. The particle densities are in agreement with those found in the literature for sandy and clayey soils [5].

Figure 4 presents results of the impact of the sampling procedure on the porosity of the soils having different textures.

As can be seen from Fig. 4, the ϕ values vary significantly for soils 1 and 2, reflecting variations on the structure of these soils resulted from sampling. A clear heterogeneity of ϕ and the occurrence of larger values in the center position (P4) of the soil samples can be observed. There is a density gradient for all soil textures similar to those reported by Pires *et al.* [13] using 2-D tomographic image analysis. The lower values of ϕ near the border of the cylinder (see Fig. 4 – positions P1 and P7) confirm the existence of compacted regions next to the edges of samples for the sandy soil (Fig. 4a). The differences in the average ϕ between P4 and P1, on the one hand, and between P4 and P7, on the other, were statistically insignificant at $P < 0.05$ probability level for soil 3; the other two soils had noticeable gradients. Although, the differences of ϕ between P4 and P1–P7 were statistically insignificant, the variation found for soil 3 is very important from the soil physical point of view. Reductions in the soil total porosity decrease its macroporosity, in size and continuity, causing little effects in microporosity [7]. This damage in the samples may affect the determination of other soil physical parameters, such as penetration resistance, water matric potential, hydraulic conductivity, etc.

The lowest variability among samples for soil 1 (see Fig. 4) is due to the fact that this type of soil can be sampled more easily than the other two soils. The largest deviations found for clayey soils may be a result of the presence of roots because these ones had been collected from surface layers in an experimental field next to a coffee plantation (soil 2) and under forest vegetation (soil 3). Pires *et al.* [14] reported a great number of regions of lower density (macropores) for the clayey soils used in the present work. The presence of these macropores can explain the largest soil variability for soils 2 and 3.

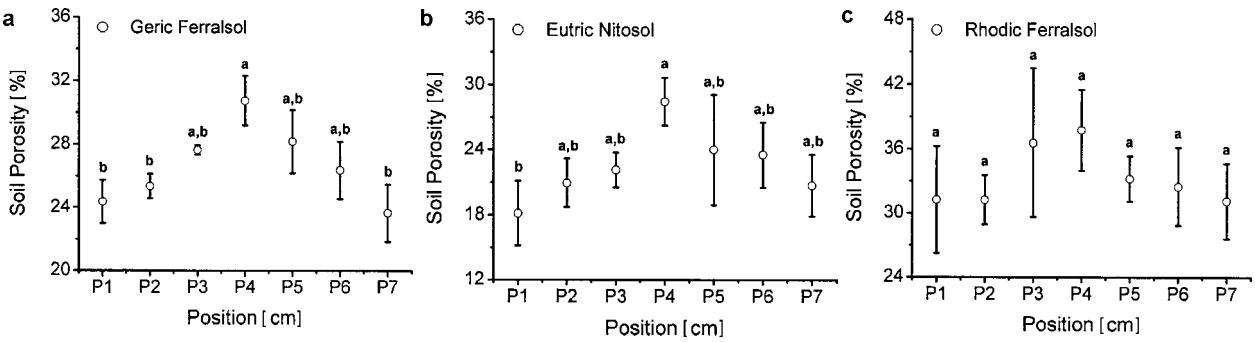

Fig. 4. Soil porosities measured in different positions (P) of the soil samples by the gamma-ray beam attenuation technique. Data represented by the same letter show subsets of the mean values that are statistically identical according to the Scheffe's test ($P < 0.05$).

Concluding remarks

It seems clear by the results that the gamma-ray attenuation technique is a valuable tool for assessing possible variations on soil structure due to the sampling procedure and for indicating that distinct soil textures can exhibit differences in the quality of collected soil samples. The largest average soil porosity reduction between the center and the edges of samples occurred for soil 2, followed by soils 1 and 3. Although, soil compactibility will be the highest for loamy textures, the largest average ϕ reduction for soil 2 may be due to the number of impacts (approximately 10) to introduce the cylinder into the soil surface. However, it is very important to pay particular attention that the possible damages on soil structure are mainly related to the soil moisture at sampling and, because of this, the percentage of the soil porosity reduction for the different soils used in this experiment can vary at each sampling.

Acknowledgment The authors wish to thank FAPESP (Grant No. 02/05066-5) for the financial support.

References

1. Appoloni CR, Rios EA (1994) Mass attenuation coefficients of Brazilian soils in the range 10–1450 KeV. Appl Radiat Isot 45:287–291
2. Coppola M, Reiniger P (1974) Influence of the chemical composition on the gamma-ray attenuation by soils. Soil Sci 117:331–335
3. Ferraz ESB, Mansell RS (1979) Determining water content and bulk density of soil by gamma-ray attenuation methods. IFAS, Florida, pp 1–51
4. Flint AL, Flint LE (2002) The solid phase: Particle density. In: Dane JH, Topp GC (eds) Methods of soil analysis. Part 4: Physical methods. Soil Sci Soc Am Book Series, vol. 5. Madison, pp 229–240
5. Grohmann F (1960) Distribuição do tamanho de poros em treˆs tipos de solos do Estado de São Paulo. Bragantia 19:319–328
6. Helsel DR, Hirsch RM (eds) (1992) Statistical methods in water resources. Elsevier, New York
7. Hillel D (ed) (1982) Introduction to soil physics. Academic Press, San Diego
8. Jenkins R, Gould RW, Gedcke D (eds) (1981) Quantitative X-ray spectrometry. Marcel Dekker Inc., New York
9. Kutílek M, Nielsen DR (eds) (1994) Soil hydrology. Catena Verlag, Reiskirchen
10. Oliveira JCM, Appoloni CR, Coimbra MM *et al*. (1998) Soil structure evaluated by gamma-ray attenuation. Soil Till Res 48:127–133
11. Pagliai M, Rousseva S, Vignozzi N *et al*. (1999) Tillage impact on soil quality. I. Soil porosity and related physical properties. Ital J Agron 2:11–20
12. Phogat VK, Aylmore LAG (1989) Evaluation of soil structure by using computer-assisted tomography. Aust J Soil Res 27:313–323
13. Pires LF, Bacchi OOS, Reichardt K (2004) Damage to soil physical properties caused by soil sampler devices as assessed by gamma-ray computed tomography. Aust J Soil Res 42:857–863
14. Pires LF, Bacchi OOS, Reichardt K (2005) Gamma-ray computed tomography to evaluate wetting/drying soil structure changes. Nucl Instrum Meth B 229:443–456
15. Pottker WE, Appoloni CR (2001) Measurement of amorphous materials porosity by gamma-ray transmission methodology. Radiat Phys Chem 61:535–536
16. Vanden Bygaart AJ, Protz R (1999) The representative elementary area (REA) in studies of quantitative soil micromorphology. Geoderma 89:333–346
17. Vomocil JA (1954) *In situ* measurement of bulk density of soil by gamma absorption technique. Soil Sci 77:341–342